

МАТЕМАТИКАЛЫҚ ҒЫЛЫМДАР
MATHEMATICAL SCIENCES
МАТЕМАТИЧЕСКИЕ НАУКИ

UDC 517.958:533.7; 532.517.4

IRSTI 27.35.17; 30.17.27

<https://doi.org/10.55452/1998-6688-2024-21-4-107-123>

^{1*}Manapova A.,

Master of applied mathematics and computer science, ORCID ID: 0000-0003-1548-7061,

*e-mail: manapova.a.k.math@gmail.com

²Beketayeva A.,

Doctor of Physical and Mathematical Sciences, ORCID ID: 0000-0003-4360-3728,

e-mail: azimaras10@gmail.com

^{3,4}Makarov V.

Candidate of Technical Sciences, ORCID ID: 0000-0003-4874-5418,

e-mail: makfone@mail.ru

¹Civil aviation academy, Almaty, Kazakhstan

²Institute of mathematics and mathematical modeling, Almaty, Kazakhstan

³Institute of control sciences RAS, Moscow, Russia

⁴National research nuclear university «MEPhI», Moscow, Russia

**PENALTY FUNCTION METHOD FOR MODELING
OF CYLINDER FLOW WITH SUBSONIC COMPRESSIBLE FLOW**

Abstract

Numerical modelling of compressible flows around moving solids is important for engineering applications such as aerodynamic flutter, rocket engines and landing gear. The penalty function method is particularly effective when using orthogonal structural meshes within a finite difference scheme and is widely used to solve both laminar and turbulent flow problems. The method is based on the direct application of the Navier-Stokes equations with added sources, which allows the boundary conditions to be set indirectly. This method facilitates the imposition of Dirichlet boundary conditions but complicates the application of Neumann conditions. Nevertheless, the method works well with both types of boundary conditions, making it suitable for thermal and compressible flows where Neumann conditions are often used. Despite its flexibility, the method requires a high degree of data management and additional coding. This paper presents results of a recently developed higher-order method for compressible subsonic flows, demonstrating accurate modeling of moving objects without numerical noise. The method has been tested on stationary and moving objects over a wide range of Reynolds and Mach numbers.

Key words: numerical modelling, cylinder, subsonic flow, penalty function method, Navier-Stokes equations system.

Introduction

In recent decades, quantitative methods have been an integral part of research in aerodynamics and fluid dynamics. One of the most important tasks is the accurate simulation of flow around various bodies, which allows predicting aerodynamic performance and optimizing designs [1–2]. One of the classical problems in this field is the modeling of flow around a cylindrical type body with supersonic flow. This process is complex and involves many physically important phenomena such as flow separation, vortex formation, and interaction of vortices with the body surface [3].

The penalty function method based on characteristics offers an effective method for solving problems with complex boundary conditions [4–7]. The main advantage of this method is its ability to take into account the influence of boundary conditions on the flow distribution, which plays a particularly important role in modeling the rotation of complex-shaped bodies. The penalty function method has been successfully applied in various areas of fluid and gas mechanics, but its use for modeling supersonic flow around a cylinder requires additional research and adaptation [8–9].

To solve the modeling problem with subsonic flows around a cylindrical-type body using the method of penalty functions based on observations, it is necessary to first determine the geometric parameters of the object and the flow properties. Then an appropriate numerical method must be selected and boundary conditions must be set [10–11]. Then, the Navier-Stokes equations describing the motion of liquid or gas in the flow are solved. In these equations, parameters such as viscosity and density of the medium have a significant influence on the characteristics of the simplified body, including the effect of force and pressure distribution [12–15]. Variation of these parameters can lead to different flow regimes, such as laminar or turbulent, which significantly affect the aerodynamic properties of the object [16–18].

Abalakin's paper presents a method of numerical modeling of external flow of solids with viscous compressible fluid, which does not require calculation of their boundaries on a computational grid. The mathematical model is solved by the method of immersed boundaries. It satisfies the necessary boundary conditions at the interface of two media (solid and air) and does not require the construction of the corresponding body grids for numerical calculations. In this work, several variants of the method are performed, corresponding to different boundary conditions for the temperature at the resistive surface in the flow: isothermal and adiabatic. In the first case, the Brinkman penalty method was applied; in the second case, the volume penalty method based on the characteristics [19–20] was applied.

The Smokoski paper used a penalty function method based on the description of body traversal by compressible viscous flows. The paper used AMR (adaptive mesh refinement) meshes [21].

The following paper by Abalakin provides a characterization-based volume determination method for numerical simulation of flow that compresses above solid resistances in unstructured grids. The aerodynamic flow modeling is based on lattices mounted under the body with rigid and fluid interfaces defined by the lattice nodes, where the boundary conditions are explicitly specified [22].

The purpose of this work is to model subsonic flows around a cylindrical body using the observation-based penalty function method. The advantages of this method include the simplicity of its implementation and the possibility of using it in different types of problems. In addition, this method can be effective in eliminating instabilities or peculiarities in the numerical solution that may arise during modeling.

For numerical solution of modeling of supersonic flow of compressible ideal gas around a cylindrical body (see Fig. 1), the application of the method of penalty functions based on observations is considered. This method allows us to efficiently solve computational fluid dynamics problems taking into account penalty functions for exact compliance with boundary conditions. The mathematical

formulation of the problem involves modifying the Navier-Stokes equations to introduce penalty functions and using the characteristics for numerical solution.

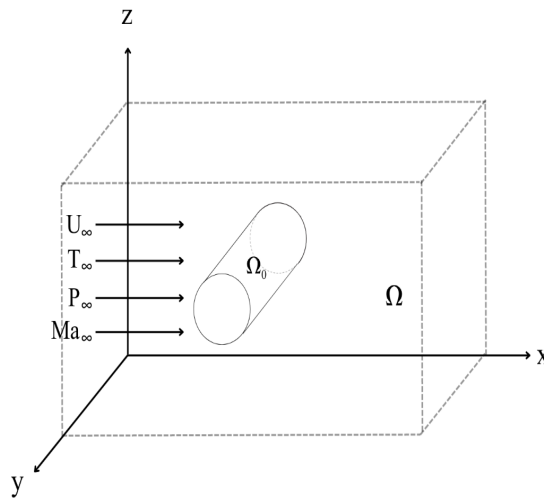


Figure 1 – Flow scheme

Main equations for a compressible perfect gas:

$$\frac{\partial \rho u_i}{\partial t} = \frac{\partial(\rho u_i u_j)}{\partial x_j} - \frac{\partial \rho}{\partial x_j} + \frac{1}{Re} \cdot \frac{\partial \tau_{ij}}{\partial x_j} = RHS_{u_j}, \quad (2)$$

$$\frac{\partial E_t}{\partial t} = - \frac{\partial(E_t + P)u_j}{\partial x_j} + \frac{1}{Re} \cdot \frac{\partial(u_i \tau_{ij})}{\partial x_j} + \frac{1}{(\gamma-1)RePr} \cdot \frac{\partial}{\partial x_j} \left(\mu \frac{\partial T}{\partial x_j} \right), \quad (3)$$

$$\tau_{ij} = \mu \left(\frac{\partial u_i}{\partial x_j} + \frac{\partial u_j}{\partial x_i} - \frac{2}{3} \frac{\partial u_k}{\partial x_k} \delta_{ij} \right),$$

$$\mu = \frac{1+S_1}{T+S_1} \cdot T^{3/2}.$$

Total energy

$$E_t = \rho e + \frac{1}{2} \rho \vec{V}^2. \quad (4)$$

Initial energy

$$e = c_V T.$$

Specific heat capacity at constant velocity

$$c_V = \frac{1}{\gamma(\gamma-1)M_\infty^2}.$$

Pressure

$$P = (\gamma - 1)\rho e = (\gamma - 1) \cdot \left[E_t - \frac{1}{2} \rho \vec{V}^2 \right].$$

Temperature

$$T = \frac{1}{\rho c_V} \left[E_t - \frac{1}{2} \rho \vec{V}^2 \right].$$

Boundary conditions for gas dynamics:

- ◆ at the input will $u_\infty, v_\infty, w_\infty, \mu_\infty, T_\infty, \rho_\infty$;
- ◆ at the output will boundary conditions of non-reflection;
- ◆ at the lateral boundaries will non-reflection conditions.

Materials and methods

The Control Based Volume Penalisation Method (CBVP) is based on the idea of introducing a penalty term into the Navier-Stokes equations (1)–(3) to model solids in fluid flow.

The basic idea of the method is that when $\eta \rightarrow 0$, the velocity of the fluid inside the solid tends to the velocity of the solid.

Comparison of CBVP with the Immersed Boundary Method (IBM) for the cylinder flow problem:

1. CBVP generally provides better accuracy near the solid boundary because the penalty term directly affects the velocity field.
2. CBVP may be more stable for larger values of the penalty parameter η , but this may lead to stiffness of the system of equations.
3. IBM can be more computationally efficient, especially for complex geometries, as it does not require mesh rebuilding.
4. CBVP is easier to realise as it does not require special processing of the solid boundary.
5. The CBVP can be easily integrated for the Navier-Stokes equations by adding a penalty term.
6. CBVP does not require complex processing of the cylinder boundary or rearrangement of the computational grid. The geometry of the cylinder is taken into account through the characteristic function $\chi(x)$, which simplifies the implementation of the method.
7. The method is easily adaptable to different flow conditions and geometries. You can easily change cylinder parameters (size, position) or add other objects to the flow.
8. If the penalty parameter η is properly chosen, the method provides a stable solution even at high Reynolds numbers.
9. The penalty term in CBVP has a clear physical interpretation as a force acting on the fluid from a solid body.
10. When the penalty parameter η is reduced, the CBVP solution converges to the exact solution of the streamline problem with the sticking condition on cylinder surface.

As we have realised, both methods give results close to the experimental value, but CBVP in this case shows a slightly more accurate result.

The CBVP method is a powerful tool for modelling the interaction of liquid and gas with solids. It provides good accuracy and is relatively easy to implement. However, like any method, it has its limitations and areas of application where it may be less effective than other approaches. The choice between CBVP and other methods depends on the specific problem, required accuracy and computational resources.

According to the paper, we consider the construction of CBVPM with positive Robin, Neumann, Dirichlet boundary conditions on a streamlined body by introducing additional penalty functions in the initial equations. For this purpose, in the region Ω with streamlined bodies Ω_0 we consider the following evolution equation for velocity [3]:

$$\frac{\partial \vec{u}}{\partial t} = RHS, \quad (6)$$

here RHS is the right-hand side describing the physical source terms. Equation (6) can be either hyperbolic or parabolic. For this problem we consider 3 main boundary conditions on the body Ω_0 :

- ♦ Dirichlet's condition is $\vec{u} = \vec{u}_0(\vec{x}, t), \vec{x} \in \partial\Omega_0$.
- ♦ Neumann's condition is $\frac{\partial \vec{u}}{\partial n} = \vec{q}(\vec{x}, t), \vec{x} \in \partial\Omega_0$;
- ♦ Robin's condition is $\alpha(\vec{x}, t)\vec{u} + \beta \frac{\partial \vec{u}}{\partial n} = \vec{q}(\vec{x}, t)$.

In order to add these boundary conditions to equation (6), we introduce the characteristic function $\kappa(\vec{x}, t)$:

$$\kappa(\vec{x}, t) = \begin{cases} 1, & \text{if } \vec{x} \in \Omega_0, \text{ inside the body} \\ 0, & \text{if } \vec{x} \notin \Omega_0 \end{cases}.$$

Then for each task according to CBVPM, equation (6) will take the following form:

$$\frac{\partial \vec{u}}{\partial t} = (1 - \kappa) \cdot RHS - \frac{\kappa}{\eta_b} (\vec{u} - \vec{u}_0) + \kappa \cdot \nu_n \cdot \frac{\partial^2 \vec{u}}{\partial x_i \partial x_i}, \quad (7)$$

$$\frac{\partial \vec{u}}{\partial t} = (1 - \kappa) \cdot RHS - \frac{\kappa}{\eta_c} \left(n_k \frac{\partial \vec{u}}{\partial x_k} - \vec{q}(\vec{x}, t) \right), \quad (8)$$

$$\frac{\partial \vec{u}}{\partial t} = (1 - \kappa) \cdot RHS - \frac{\kappa}{\eta_c} \left[\alpha(\vec{x}, t) \vec{u} + \beta \cdot n_k \cdot \frac{\partial \vec{u}}{\partial n} - \vec{q}(\vec{x}, t) \right], \quad (9)$$

here η_b, η_c are penalty parameters, which a $\eta_b, \eta_c \rightarrow 0$ controls the error of decisions by reducing the time in the calculation of penalty functions.

Since the basic system (1)–(4) contains the variables $\rho, \rho \vec{u}_i$ it is necessary to define the corresponding equations with penalty functions for the density. It is necessary to preserve the continuity equation inside the streamlined body. According to the paper, consider such a passive evolutionary condition, which is based on Neumann's condition. Due to the fact that the flow characteristics are directed inside the streamlined body, the solution at the interface should be determined by the flow physics using some derivative defined by the penalty function in the region Ω_0 [3].

In this paper, the Neumann condition for ρ is used, where the derivative sought in the region Ω_0 will be the derivative along the normal to the body surface, and the density inside the body becomes passive to the gas flow.

This procedure can be carried out by introducing an additional equation and taking advantage of the hyperbolicity of the CBVPM equations to extrapolate the density derivative to the surface of the streamlined body along the normal by means of the following equation:

$$\frac{\partial \Phi}{\partial t} = \frac{\kappa}{\eta_c} n_k \frac{\partial \Phi}{\partial x_k}, \quad (10)$$

$$\Phi = (1 - \kappa) n_k \frac{\partial \rho}{\partial x_k} + \varphi \Phi,$$

$$\Phi|_{\Omega_0} = \frac{\partial \rho}{\partial n}.$$

Finding $\Phi(\vec{x}, t)$ along the Ω_0 region provides the necessary boundary condition from ρ for equation (7), which is solved only inside the body. Thus, the density derivatives outside the body are determined from the continuity equation and extrapolated inside the body by integrating equation (7). Therefore, the function $\Phi(\vec{x}, t)$ is completely passive to the physics of the flow.

Then the equation for the density with the penalty function taking into account the Neumann boundary condition for ρ at the boundary of the streamlined body is written as follows:

$$\frac{\partial \rho}{\partial t} = (1 - \kappa) \cdot RHS - \frac{\kappa}{\eta_c} \left(n_k \frac{\partial \rho}{\partial x_k} - \Phi \right), \quad (11)$$

where RHS is the right-hand side of the continuity equation.

Using the constructed equations with penalty functions for \vec{u} , $\vec{\rho}$ we can write equations for \vec{u} and E_t using the following equations:

$$\frac{\partial \rho \vec{u}_i}{\partial t} = \vec{u} \frac{\partial \rho}{\partial t} + \rho \frac{\partial \vec{u}}{\partial t}, \tag{12}$$

$$\frac{\partial E_t}{\partial t} = \frac{\partial}{\partial t} \left(\rho \zeta T + \frac{1}{2} \vec{u}_i^2 \right) = \frac{\partial}{\partial t} (\rho e), \tag{13}$$

where $e = \zeta T + \frac{1}{2} \vec{u}_i^2$.

$$\begin{aligned} \frac{\partial (\rho e)}{\partial t} &= e \frac{\partial \rho}{\partial t} + \rho \frac{\partial e}{\partial t} = e \frac{\partial \rho}{\partial t} + \rho \left[\frac{\partial}{\partial t} \zeta T + \frac{\partial}{\partial t} \left(\frac{1}{2} \vec{u}_i^2 \right) \right] = \\ &= e \frac{\partial \rho}{\partial t} + \rho \vec{u}_i \frac{\partial u}{\partial t} + c_V \frac{\partial T}{\partial t}. \end{aligned}$$

Boundary conditions are set for the temperature on the streamlined body:

$$n_k \frac{\partial T}{\partial x_k} |_{\partial \Omega_0} = q.$$

The modified equation for the temperature for the whole region is written as:

$$\frac{\partial T}{\partial t} = (1 - \kappa) \cdot RHS - \frac{\kappa}{\eta_c} \left(n_k \frac{\partial T}{\partial x_k} - q \right). \tag{14}$$

where M_∞ is Mach number, $Re = \frac{u_\infty L \rho}{\mu}$ is Reynolds number, Pr is Prandtl number.

Let us rewrite (12) taking into account (7) and (11):

$$\begin{aligned} \frac{\partial \rho \vec{u}_i}{\partial t} &= \vec{u}_i \frac{\partial \rho}{\partial t} + \rho \frac{\partial \vec{u}_i}{\partial t} = \vec{u}_i (1 - \kappa) \cdot RHS - \frac{\vec{u}_i \kappa}{\eta_c} \left(n_k \frac{\partial \rho}{\partial x_k} - \Phi \right) + \rho (1 - \kappa) \cdot RHS - \frac{\kappa \rho}{\eta_b} (\vec{u} - \vec{u}_0) + \rho \kappa \cdot \\ v_n \cdot \frac{\partial^2 \vec{u}_i}{\partial x_i \partial x_i} &= (1 - \kappa) \cdot [\vec{u}_i RHS + \rho \cdot RHS] - \left[\frac{\vec{u}_i \kappa}{\eta_c} \left(n_k \frac{\partial \rho}{\partial x_k} - \Phi \right) + \rho \frac{\kappa}{\eta_b} (\vec{u} - \vec{u}_0) + \rho \kappa \cdot v_n \cdot \frac{\partial^2 \vec{u}_i}{\partial x_i \partial x_i} \right]. \end{aligned}$$

Now let us rewrite (13) taking into account (11), (7) and (14):

$$\begin{aligned} \frac{\partial E_t}{\partial t} &= e (1 - \kappa) \cdot RHS - \frac{e \kappa}{\eta_c} \left(n_k \frac{\partial \rho}{\partial x_k} - \Phi \right) + \rho \vec{u}_i (1 - \kappa) \cdot RHS - \rho \vec{u}_i \frac{\kappa}{\eta_b} (\vec{u} - \vec{u}_0) + \rho \vec{u}_i \kappa \cdot v_n \cdot \\ \frac{\partial^2 \vec{u}_i}{\partial x_i \partial x_i} &+ c_V \rho (1 - \kappa) RHS - \frac{c_V \rho \kappa}{\eta_c} \left(n_k \frac{\partial T}{\partial x_k} - q \right) = (1 - \kappa) \cdot [e RHS + \rho \vec{u}_i \cdot RHS + c_V \rho \cdot RHS] - \\ \frac{e \kappa}{\eta_c} \left(n_k \frac{\partial T}{\partial x_k} - \Phi \right) &- \rho \vec{u}_i \frac{\kappa}{\eta_b} (\vec{u} - \vec{u}_0) + \rho \vec{u}_i \kappa \cdot v_n \cdot \frac{\partial^2 \vec{u}_i}{\partial x_i \partial x_i} - \frac{c_V \rho \kappa}{\eta_c} \left(n_k \frac{\partial T}{\partial x_k} - q \right) = (1 - \kappa) \cdot RHS - \\ \frac{e \kappa}{\eta_c} n_k \frac{\partial \rho}{\partial x_k} + \frac{\kappa E_t \Phi}{\eta_c \rho} &- \rho \vec{u}_i \frac{\kappa}{\eta_b} (\vec{u} - \vec{u}_0) + \rho \vec{u}_i \kappa \cdot v_n \cdot \frac{\partial^2 \vec{u}_i}{\partial x_i \partial x_i} - \frac{c_V \rho \kappa}{\eta_c} \left(n_k \frac{\partial T}{\partial x_k} - q \right) = (1 - \kappa) \cdot RHS - \\ \left[\frac{n_k}{\eta_c} \left(\frac{\partial \rho e}{\partial x_k} - \rho \frac{\partial e}{\partial x_k} \right) + \rho \vec{u}_i \frac{\kappa}{\eta_b} (\vec{u} - \vec{u}_0) + \rho \vec{u}_i \kappa \cdot v_n \cdot \frac{\partial^2 \vec{u}_i}{\partial x_i \partial x_i} - \frac{1}{\eta_c} \frac{E_t \Phi}{\rho} - \frac{c_V \rho}{\eta_c} \left(n_k \frac{\partial T}{\partial x_k} - q \right) \right] &= (1 - \kappa) \cdot \\ RHS - \left[\frac{n_k}{\eta_c} \frac{\partial E_t}{\partial x_k} - \frac{n_k}{\eta_c} \rho \left(\frac{\partial c_V T}{\partial x_k} + \frac{\partial}{\partial t} \left(\frac{1}{2} \vec{u}_i^2 \right) \right) + \frac{\rho \vec{u}_i}{\eta_b} (\vec{u} - \vec{u}_0) + \rho \vec{u}_i \cdot v_n \cdot \frac{\partial^2 \vec{u}_i}{\partial x_i \partial x_i} - \frac{1}{\eta_c} \frac{E_t \Phi}{\rho} - \frac{c_V \rho}{\eta_c} n_k \frac{\partial T}{\partial x_k} - \right. \\ \left. \frac{c_V \rho q}{\eta_c} \right] &= (1 - \kappa) \cdot RHS - \kappa, \\ \left[\frac{n_k}{\eta_c} \frac{\partial E_t}{\partial x_k} - \frac{2 n_k c_V \rho}{\eta_c} \frac{\partial T}{\partial x_k} - \frac{n_k \rho \vec{u}_i}{\eta_c} \frac{\partial \vec{u}_i}{\partial x_k} + \frac{\rho \vec{u}_i}{\eta_b} (\vec{u} - \vec{u}_0) + \rho \vec{u}_i \cdot v_n \cdot \frac{\partial^2 \vec{u}_i}{\partial x_i \partial x_i} - \frac{1}{\eta_c} \frac{E_t \Phi}{\rho} - \frac{c_V \rho q}{\eta_c} \right] &= (1 - \kappa) \cdot RHS - \\ \kappa \cdot \left[\frac{\eta_k}{\eta_c} \frac{\partial E_t}{\partial x_k} - \frac{2 \eta_k c_V \rho}{\eta_c} \frac{\partial T}{\partial x_k} - \frac{\eta_k \rho \vec{u}_i}{\eta_c} \frac{\partial \vec{u}_i}{\partial x_k} + \frac{\rho \vec{u}_i}{\eta_b} (\vec{u} - \vec{u}_0) + \rho \vec{u}_i \cdot v_n \cdot \frac{\partial^2 \vec{u}_i}{\partial x_i \partial x_i} - \frac{1}{\eta_c} \frac{E_t \Phi}{\rho} - \frac{c_V \rho q}{\eta_c} \right], \end{aligned}$$

Let $q=0$ in this problem, i.e. $\eta_k \frac{\partial \Gamma}{\partial x_k} = q = 0$, then the energy equation is rewritten as:

$$\frac{\partial E_t}{\partial t} = (1 - \kappa) \cdot RHS - \kappa \cdot \left[\frac{\eta_k}{\eta_c} \frac{\partial E_t}{\partial x_k} + \frac{\rho \bar{u}_i}{\eta_b} \cdot (\bar{u} - \bar{u}_o) - \frac{\eta_k \rho \bar{u}_i}{\eta_c} \cdot \frac{\partial \bar{u}_i}{\partial x_k} - \frac{1}{\eta_c} \frac{E_t \Phi}{\rho} + \rho \bar{u}_i v_n \cdot \frac{\partial^2 \bar{u}_i}{\partial x_i \partial x_i} \right]$$

Let us write the final modified system of equations (1)-(3) taking into account the penalty functions, decreasing boundary conditions on the streamlined body:

$$\left\{ \begin{array}{l} \frac{\partial \rho}{\partial t} = (1 - \kappa) \cdot RHS - \frac{\kappa}{\eta_c} (n_k \frac{\partial \rho}{\partial x_k} - \Phi) \\ \frac{\partial \rho \bar{u}_i}{\partial t} = (1 - \kappa) \cdot RHS - \kappa \left[\frac{1}{\eta_b} \cdot \rho (\bar{u}_i - \bar{u}_o) + \frac{\bar{u}_i}{\eta_c} (n_k \frac{\partial \rho}{\partial x_k} - \Phi) - \rho v_n \cdot \frac{\partial^2 \bar{u}_i}{\partial x_j \partial x_j} \right] \\ \frac{\partial E_t}{\partial t} = (1 - \kappa) \cdot RHS - \kappa \cdot \left[\frac{\eta_k}{\eta_c} \frac{\partial E_t}{\partial x_k} + \frac{\rho \bar{u}_i}{\eta_b} \cdot (\bar{u}_i - \bar{u}_o) - \frac{\rho \bar{u}_i}{\eta_c} \cdot n_k \frac{\partial \bar{u}_i}{\partial x_k} - \frac{1}{\eta_c} \frac{E_t \Phi}{\rho} + \rho \bar{u}_i v_n \cdot \frac{\partial^2 \bar{u}_i}{\partial x_j \partial x_j} \right] \end{array} \right.$$

In the obtained system, let us represent the RHS as a sum of convective and viscous summands, then:

$$\left\{ \begin{array}{l} \frac{\partial \rho}{\partial t} + (1 - \kappa) \cdot \frac{\partial \rho \bar{u}_i}{\partial x_i} + (1 - \kappa) RHS + \frac{\kappa}{\eta_c} (n_k \frac{\partial \rho}{\partial x_k} - \Phi) = 0 \\ \frac{\partial \rho \bar{u}_i}{\partial t} + (1 - \kappa) \cdot \frac{\partial \rho u_i u_j}{\partial x_j} + (1 - \kappa) RHS_v + \kappa \left[\frac{\rho}{\eta_b} (\bar{u}_i - \bar{u}_o) + \frac{\bar{u}_i}{\eta_c} (n_k \frac{\partial \rho}{\partial x_k} - \Phi) \right] - \kappa \left[\rho v_n \cdot \frac{\partial^2 \bar{u}_i^2}{\partial x_j \partial x_j} \right] = 0 \\ \frac{\partial E_t}{\partial t} + (1 - \kappa) \frac{\partial u_i E_t}{\partial x_j} + (1 - \kappa) RHS_v + \kappa \left[\frac{\rho u_i}{\eta_b} (\bar{u}_i - \bar{u}_o) + \frac{n_k}{\eta_c} \frac{\partial E_t}{\partial x_k} - \frac{\rho \bar{u}_i}{\eta_c} \cdot n_k \frac{\partial \bar{u}_i}{\partial x_k} - \frac{E_t \Phi}{\eta_c \rho} + \rho \bar{u}_i v_n \cdot \frac{\partial^2 \bar{u}_i}{\partial x_j \partial x_j} \right] = 0. \end{array} \right.$$

Now let us group the terms in the equations that are included in the vectors of variables \bar{u} and κ_i :

$$\left\{ \begin{array}{l} \frac{\partial \rho}{\partial t} + (1 - \kappa) \cdot \frac{\partial \rho \bar{u}_i}{\partial x_i} + (1 - \kappa) RHS + \kappa_c n_k \frac{\partial \rho}{\partial x_k} - \kappa_c \Phi = 0 \\ \frac{\partial \rho \bar{u}_i}{\partial t} + (1 - \kappa) \cdot \frac{\partial \rho u_i u_j}{\partial x_j} + (1 - \kappa) RHS_v + \kappa_c n_k \frac{\partial \rho u_i}{\partial x_k} - \kappa_c n_k \rho \frac{\partial u_j}{\partial x_k} + \kappa_b \rho (\bar{u}_i - \bar{u}_{oi}) - \kappa_c u_i \Phi - \kappa \rho v_n \cdot \frac{\partial^2 u_i}{\partial x_j \partial x_j} = 0 \\ \frac{\partial E_t}{\partial t} + (1 - \kappa) \cdot \frac{\partial \bar{u}_i \vec{E}_t}{\partial x_j} + (1 - \kappa) RHS_v + \kappa_c \cdot n_k \cdot \frac{\partial E_t}{\partial x_k} + \kappa_b \rho \bar{u}_i \cdot (\bar{u}_i - \bar{u}_o) - \kappa_c \cdot \frac{E_t}{\rho} \Phi - \kappa_c \cdot \rho \bar{u}_i n_k \cdot \frac{\partial \bar{u}_i}{\partial x_k} + \kappa v_n \rho u_i \cdot \frac{\partial^2 \bar{u}_i}{\partial x_j \partial x_j} = 0 \\ \kappa_c = \frac{\kappa}{\eta_c}, \kappa_b = \frac{\kappa}{\eta_b}. \end{array} \right.$$

Let us rewrite (14) in vector form:

$$\frac{\partial \bar{u}}{\partial t} + (I - \kappa) \cdot \left(\frac{\partial \vec{E}}{\partial x} + \frac{\partial \vec{F}}{\partial y} + \frac{\partial \vec{G}}{\partial z} \right) + \kappa_{cn} n_k \frac{\partial \bar{u}}{\partial x_k} + \vec{S} + (1 - \kappa) \cdot RHS = 0. \quad (15)$$

here the vectors \vec{E} , \vec{F} , \vec{G} and \vec{S} take the following form:

$$\vec{S} = \begin{bmatrix} \kappa_b \rho (u - u_0) - \kappa_c \Phi u - \kappa_c n_k \rho \frac{\partial u}{\partial x_k} - \kappa \rho v_n \cdot \frac{\partial^2 u}{\partial x^2} \\ \kappa_b \rho (v - v_0) - \kappa_c \Phi v - \kappa_c n_k \rho \frac{\partial v}{\partial x_k} - \kappa \rho v_n \cdot \frac{\partial^2 v}{\partial y^2} \\ \kappa_b \rho (w - w_0) - \kappa_c \Phi w - \kappa_c n_k \rho \frac{\partial w}{\partial x_k} - \kappa \rho v_n \cdot \frac{\partial^2 w}{\partial z^2} \\ \kappa_b [\rho u (u - u_0) + \rho v (v - v_0) + \rho w (w - w_0)] - \kappa_c \Phi \frac{E_t}{\rho} - \kappa_c \cdot n_k \left\{ \rho \frac{\partial u}{\partial x_k} + \rho \frac{\partial v}{\partial x_k} + \rho \frac{\partial w}{\partial x_k} \right\} - \kappa \rho v_n \left\{ u \frac{\partial^2 u}{\partial x^2} + v \frac{\partial^2 v}{\partial y^2} + w \frac{\partial^2 w}{\partial z^2} \right\} \end{bmatrix}$$

Let us rewrite (15) taking into account the new vector S^n :

$$\frac{\partial \vec{u}}{\partial t} + (I - \kappa) \cdot \left(\frac{\partial \vec{E}}{\partial x} + \frac{\partial \vec{F}}{\partial y} + \frac{\partial \vec{G}}{\partial z} \right) + \kappa_{c_n} n_k \frac{\partial \vec{u}}{\partial x_k} + \kappa_{b_n} (\vec{u}_i - \vec{u}_{oi}) + S^n + (1 - \kappa) \cdot RHS = 0, \quad (17)$$

where

$$\kappa_{b_n} = \begin{bmatrix} 0 & 0 & 0 & 0 & 0 \\ 0 & \frac{x}{\kappa_b} & 0 & 0 & 0 \\ 0 & 0 & \frac{x}{\kappa_b} & 0 & 0 \\ 0 & 0 & 0 & \frac{x}{\kappa_b} & 0 \\ 0 & 0 & 0 & 0 & 0 \end{bmatrix},$$

$$\kappa_{c_n} = \begin{bmatrix} \frac{x}{\kappa_c} & 0 & 0 & 0 & 0 \\ 0 & \frac{x}{\kappa_c} & 0 & 0 & 0 \\ 0 & 0 & \frac{x}{\kappa_c} & 0 & 0 \\ 0 & 0 & 0 & \frac{x}{\kappa_c} & 0 \\ 0 & 0 & 0 & 0 & \frac{x}{\kappa_c} \end{bmatrix},$$

$$S^n = \begin{bmatrix} -\kappa_c \Phi \\ -\kappa_c \Phi u - \kappa_c n_k \rho \frac{\partial u}{\partial x_k} - \kappa \rho v_n \cdot \frac{\partial^2 u}{\partial x^2} \\ -\kappa_c \Phi v - \kappa_c n_k \rho \frac{\partial v}{\partial x_k} - \kappa \rho v_n \cdot \frac{\partial^2 v}{\partial y^2} \\ -\kappa_c \Phi w - \kappa_c n_k \rho \frac{\partial w}{\partial x_k} - \kappa \rho v_n \cdot \frac{\partial^2 w}{\partial z^2} \\ \kappa_b [\rho u(u - u_0) + \rho v(v - v_0) + \rho w(w - w_0)] - \kappa_c \Phi \frac{E_t}{\rho} - \kappa_c \cdot n_k \left\{ \rho \frac{\partial u}{\partial x_k} + \rho \frac{\partial v}{\partial x_k} + \rho \frac{\partial w}{\partial x_k} \right\} \\ -\kappa \rho v_n \left\{ u \frac{\partial^2 u}{\partial x^2} + v \frac{\partial^2 v}{\partial y^2} + w \frac{\partial^2 w}{\partial z^2} \right\} \end{bmatrix},$$

when $n_k \frac{\partial u}{\partial x_k} = \left(n_x \frac{\partial u}{\partial x} + n_y \frac{\partial u}{\partial y} + n_z \frac{\partial u}{\partial z} \right)$ is normal.

$$\vec{u} = \begin{bmatrix} \rho \\ \rho u \\ \rho v \\ \rho w \\ E_t \end{bmatrix}, \quad \vec{E} = \begin{bmatrix} \rho u \\ \rho u^2 + p \\ \rho uv \\ \rho uw \\ (E_t + p)u \end{bmatrix}, \quad \vec{F} = \begin{bmatrix} \rho v \\ \rho uv \\ \rho v^2 + p \\ \rho vw \\ (E_t + p)v \end{bmatrix}, \quad \vec{G} = \begin{bmatrix} \rho w \\ \rho uw \\ \rho vw \\ \rho w^2 + p \\ (E_t + p)w \end{bmatrix}.$$

Then after time integration:

$$\bar{u}^{n+1} + \Delta t(I - \kappa) \cdot \left(A^n \frac{\partial \bar{u}^{n+1}}{\partial x} + B^n \frac{\partial \bar{u}^{n+1}}{\partial y} + C^n \frac{\partial \bar{u}^{n+1}}{\partial z} \right) + \Delta t \cdot \kappa_{b_n} \cdot (\bar{u}^{n+1} - \bar{u}_{oi}) = \bar{u}^n - \Delta t(I - \kappa) \cdot RHS^n - \Delta t \cdot \kappa_c \cdot n_k \cdot \frac{\partial \bar{u}}{\partial x^k} - \Delta t S^n$$

$$(I + \Delta t \kappa_{b_n}) \bar{u}^{n+1} + \Delta t(I - \kappa) \cdot \left(A^n \frac{\partial \bar{u}^{n+1}}{\partial x} + B^n \frac{\partial \bar{u}^{n+1}}{\partial y} + C^n \frac{\partial \bar{u}^{n+1}}{\partial z} \right) = \bar{u}^n + \Delta t \cdot \kappa_{b_n} \cdot \bar{u}_{oi} - \Delta t(I - \kappa) \cdot RHS^n - \Delta t \cdot \kappa_c \cdot n_k \cdot \frac{\partial \bar{u}}{\partial x^k} - \Delta t S^n | : (I + \Delta t \cdot \kappa_{b_n})$$

$$\bar{u}^{n+1} + \Delta t(I + \Delta t \kappa_{b_n})^{-1} \cdot (I - \kappa) \cdot \left(A^n \frac{\partial \bar{u}^{n+1}}{\partial x} + B^n \frac{\partial \bar{u}^{n+1}}{\partial y} + C^n \frac{\partial \bar{u}^{n+1}}{\partial z} \right) = (I + \Delta t \kappa_{b_n})^{-1} \bar{u}^n + \Delta t(I + \Delta t \cdot \kappa_{b_n})^{-1} \cdot \kappa_{b_n} \bar{u}_{oi} - \Delta t(I + \Delta t \cdot \kappa_{b_n})^{-1} (I - \kappa) \cdot RHS^n - \Delta t(I + \Delta t \cdot \kappa_{b_n})^{-1} \cdot \kappa_c \cdot n_k \cdot \frac{\partial \bar{u}^n}{\partial x^k} - \Delta t(I + \Delta t \cdot \kappa_{b_n})^{-1} S^n$$

A different integration:

$$(I + \Delta t \cdot \kappa_{b_n}) \bar{u}^{n+1} + \Delta t(I - \kappa) \left(A^n \frac{\partial \bar{u}^{n+1}}{\partial x} + B^n \frac{\partial \bar{u}^{n+1}}{\partial y} + C^n \frac{\partial \bar{u}^{n+1}}{\partial z} \right) + \Delta t \cdot \kappa_{c_n} \cdot n_k \left(\frac{\partial \bar{u}^{n+1}}{\partial x} + \frac{\partial \bar{u}^{n+1}}{\partial y} + \frac{\partial \bar{u}^{n+1}}{\partial z} \right) = \bar{u}^n - \Delta t(I - \kappa) RHS^n - \Delta t S^n$$

then

$$\Delta t \left\{ [(I - \kappa)A^n + \kappa_{c_n} \cdot n_k] \frac{\partial \bar{u}^{n+1}}{\partial x} + [(I - \kappa)B^n + \kappa_{c_n} \cdot n_y] \frac{\partial \bar{u}^{n+1}}{\partial y} + [(I - \kappa)C^n + \kappa_{c_n} \cdot n_z] \frac{\partial \bar{u}^{n+1}}{\partial z} \right\} = \bar{u}^n - \Delta t(I - \kappa) RHS^n - \Delta t S^n$$

$$A^{new} = (I - \kappa)A^n + \kappa_{c_n} \cdot n_k,$$

$$B^{new} = (I - \kappa)B^n + \kappa_{c_n} \cdot n_y,$$

$$C^{new} = (I - \kappa)C^n + \kappa_{c_n} \cdot n_z,$$

$$\bar{u}^{n+1} + (I + \Delta t \kappa_{b_n})^{-1} \Delta t \cdot \left\{ A^{new} \frac{\partial \bar{u}^{n+1}}{\partial x} + B^{new} \frac{\partial \bar{u}^{n+1}}{\partial y} + C^{new} \frac{\partial \bar{u}^{n+1}}{\partial z} \right\} = (I + \Delta t \kappa_{b_n})^{-1} \bar{u}^n - (I + \Delta t \kappa_{b_n})^{-1} \Delta t(I - \kappa) RHS^n - (I + \Delta t \cdot \kappa_{b_n})^{-1} \Delta t S^n$$

$$\frac{\partial \Phi}{\partial t} = -\frac{\kappa}{\eta_c} \eta_k \frac{\partial \Phi}{\partial x_k},$$

$$\Phi = (1 - \kappa) n_k \frac{\partial \rho}{\partial n_k} + \kappa \Phi,$$

$$\frac{\partial \Phi}{\partial t} + \frac{\kappa}{\eta_c} \cdot \left[n_x \frac{\partial \Phi}{\partial x} + n_y \frac{\partial \Phi}{\partial y} + n_z \frac{\partial \Phi}{\partial z} \right] = 0,$$

$\frac{\kappa}{\eta_c} > 0$ the approximation depends on n_x, n_y, n_z , if they are positive, the difference is backward, if they are negative, the difference is forward.

$$\frac{\partial \Phi}{\partial t} = \frac{\Phi^{n+1} - \Phi^n}{\Delta t} + O(\Delta t),$$

$$\frac{\partial \Phi}{\partial x} = \frac{\Phi_i - \Phi_{i-1}}{\Delta x} + O(\Delta x), \text{ если } \frac{\kappa}{\eta_c} > 0,$$

$$\frac{\partial \Phi}{\partial x} = \frac{\Phi_{i+1} - \Phi_i}{\Delta x} + O(\Delta x), \text{ если } \frac{\kappa}{\eta_c} < 0,$$

$$\frac{\partial^2 u}{\partial x^2} = \frac{u_{i+1} - 2u_i + u_{i-1}}{2\Delta x^2} + O(\Delta x^2),$$

$$\frac{\Phi^{n+1} - \Phi^n}{\Delta t} = -\frac{\kappa}{\eta_c} \left[n_x \frac{\partial \Phi}{\partial x} + n_y \frac{\partial \Phi}{\partial y} + n_z \frac{\partial \Phi}{\partial z} \right],$$

$$\Phi^{n+1} = \Phi^n - \frac{\Delta t \kappa}{\eta_c} \left[n_x \frac{\partial \Phi}{\partial x} + n_y \frac{\partial \Phi}{\partial y} + n_z \frac{\partial \Phi}{\partial z} \right].$$

For $\frac{\kappa}{\eta_c} > 0$:

$$\Phi^{n+1} = \Phi^n - \frac{\Delta t \kappa}{\eta_c} \left[n_x \frac{\Phi_i - \Phi_{i-1}}{\Delta x} + n_y \frac{\Phi_j - \Phi_{j-1}}{\Delta y} + n_z \frac{\Phi_k - \Phi_{k-1}}{\Delta z} \right].$$

For $\frac{\kappa}{\eta_c} < 0$:

$$\Phi^{n+1} = \Phi^n - \frac{\Delta t \kappa}{\eta_c} \left[n_x \frac{\Phi_{i+1} - \Phi_i}{\Delta x} + n_y \frac{\Phi_{j+1} - \Phi_j}{\Delta y} + n_z \frac{\Phi_{k+1} - \Phi_k}{\Delta z} \right].$$

Results and discussion

Figure 2 shows that when $M_\infty = 0.5$ and $Re = 1000$, the flow is subsonic around a cylindrical body. The image shows the distribution of Mach numbers in the rotational region of the cylinder, showing regions characterized by changes in flow velocity.

The flow collides with the cylinder, causing pressure increase and velocity deceleration in front of the cylinder. This region is represented by a smooth transition to lower values of Mach numbers. The flow rotates around the cylinder and splits into two parts, resulting in a complex velocity distribution around the cylinder. Along the surface of the cylinder, high values of Mach number are observed at which the flow accelerates. Behind the cylinder, a recirculation region or trace is formed along which the flow velocity decreases significantly. Low values of Mach numbers are seen in this region, indicating the formation of vortices and turbulent current. The formation of low-velocity vortices and regions behind the cylinder is a phenomenon characteristic of rotating bodies in subsonic flow conditions.

Figure 2 shows typical supersonic flow behavior when a cylindrical body is rotating. At $M_\infty = 0.5$, the flow velocity is half the speed of sound in this medium, which allows us to observe both flow stabilization and turbulent regions.

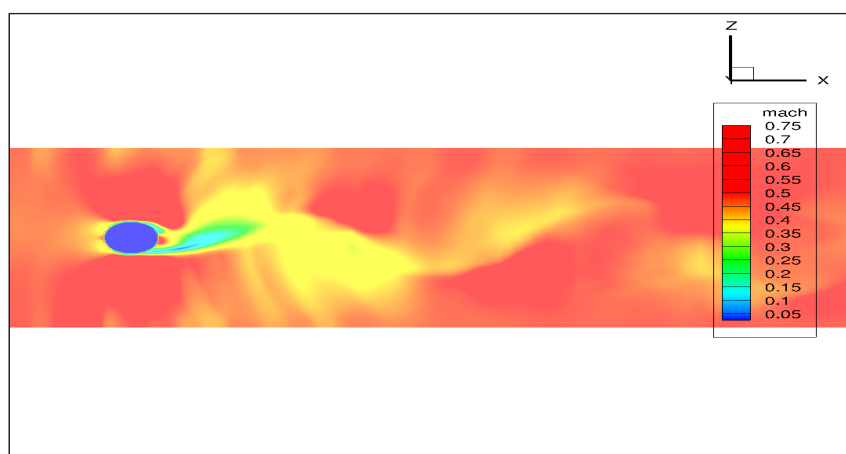
$Re = 1000$ shows an average turbulent flow regime, which is confirmed by the presence of vortices behind the cylinder.

In Figure 3, the cylindrical body causes significant disturbance in the flow, which is reflected in the change in velocities around it. Flow inhibition is observed at the front of the cylinder, resulting in a low velocity zone (dark blue color) in front of the body.

Behind the cylinder, in its shaded region, a high velocity zone characterized by a high velocity gradient is formed. This area depends on the impact of the cylinder on the surrounding flow and the formation of vortices. The vortices, in turn, create regions of variable pressure and velocity at the rear of the cylinder.



a)



b)

Figure 2 – Variation of the Mach parameter at $M_\infty = 0.5$ and $Re = 1000$

The central part shows a region of relatively constant velocity where the flow equalizes after perturbations caused by the cylinder rotation. The influence of the cylinder on the flow gradually decreases with distance from the body, and the flow velocity tends to the initial values.

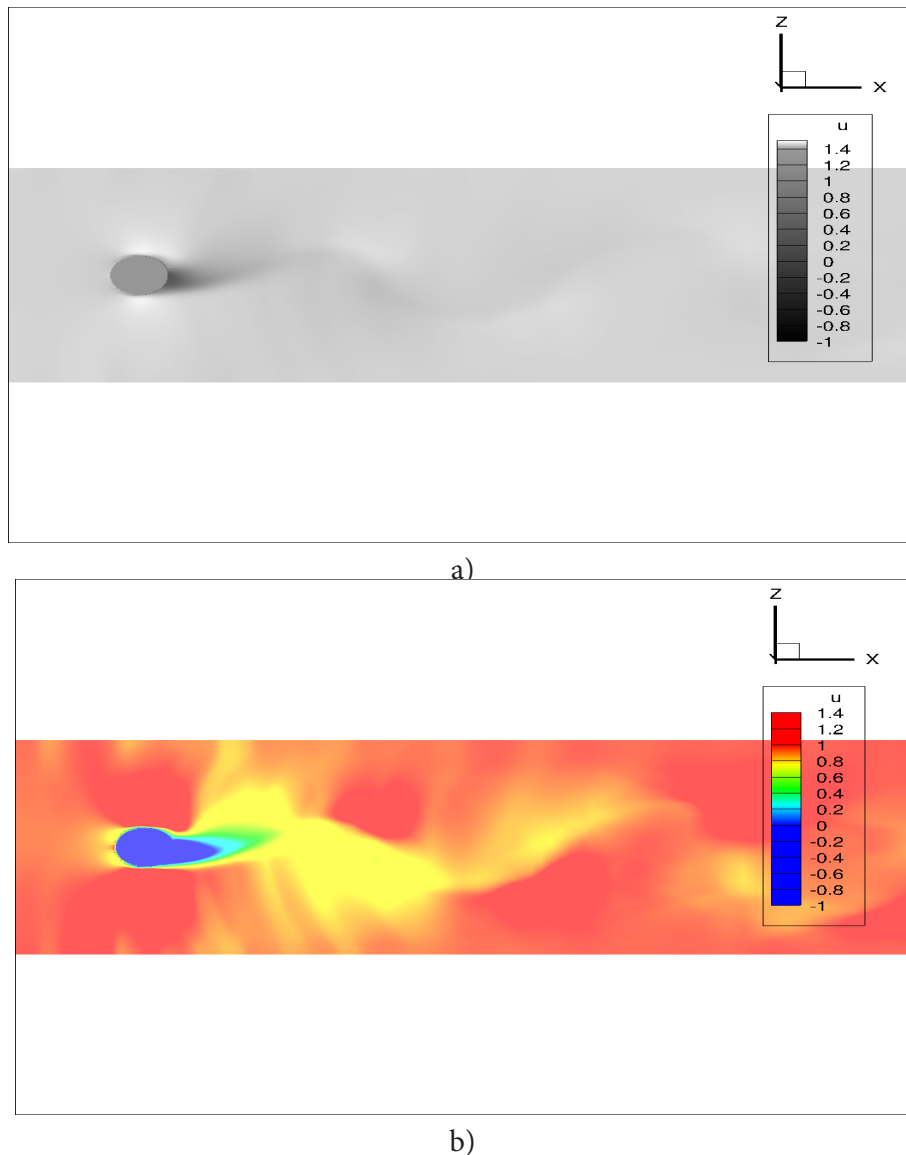


Figure 3 – Variation of velocity U at $M_\infty = 0.5$ and $Re = 1000$

Figure 4 shows the temperature change during the rotation of a cylindrical body with supersonic flow $M_\infty = 0.5$ and $Re = 1000$. The region in front of the cylinder is characterized by an increase in temperature caused by compression and deceleration of the flow. This manifests itself as a concentration at high temperatures on the front surface of the cylinder.

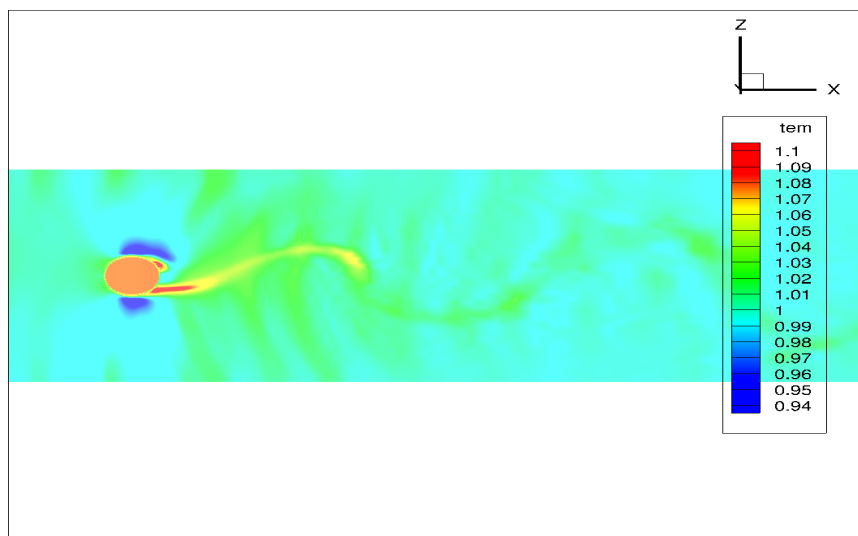
At the sides of the cylinder, the temperature gradually decreases due to leakage and opening of the flow around the body. A low temperature zone is formed at the rear of the cylinder, which is the result of vortices and turbulent mixing caused by the flow around the cylinder. These vortices promote mixing of cold and hot air, creating a low temperature zone behind the body.

Further, a gradual equalization of the temperature field can be seen from the cylinder, where the flows mix and recover their original temperature. These changes best reflect the thermal effect of the

cylinder on the surrounding flow and demonstrate the effect of heat transfer and turbulent mixing in the region behind the body.



a)



b)

Figure 4 – Temperature change T at $M_\infty = 0.5$ and $Re = 1000$

Figure 5 compares the experimental data for the pressure coefficient P at the cylinder surface. At $Re = 40$, the flow is characterized by a laminar constant recirculation zone, since the critical point of Bernard-Fon Karman instability is not reached. A qualitative comparison of the vortex isocontours with data from Al-Marouf et al [23] shows that the structural organization of the flow is well understood. This includes the pressure coefficient C_p , which agrees well with the results of Al-Marouf et al [23].

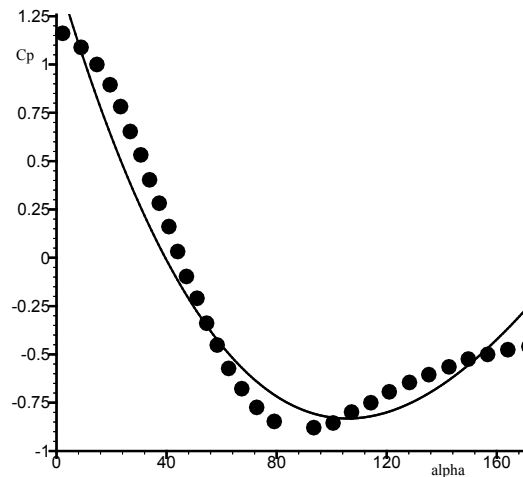


Figure 5 – The pressure coefficient C_p on the cylinder surface is a constant solution for $M_\infty = 0.05$ and $Re = 40$ (••• is experiment and — is numerical result)

Conclusion

In this work, a characteristic-based penalty function method was used to simulate the supersonic flow around a cylinder at parameters $M_\infty = 0.5$ and $Re = 1000$. The numerical simulation results were carefully compared with experimental data, which confirmed the accuracy and reliability of the proposed approach.

The use of the penalty function method based on characteristics has shown that it provides high accuracy and stability of the numerical solution when modeling complex flows. This method allowed us to effectively consider boundary conditions and flow features around the cylinder.

In addition, a new method of reducing the equations to dimensionless form was used in this work, which improved the convergence of the calculations and increased their accuracy. This application also helped to reduce the computational cost, which is an important factor when performing complex numerical calculations.

Comparison of the numerical simulation results with experimental data showed good agreement, which confirmed the correctness of the selected method and its application for solving aerodynamic problems at supersonic speeds. An ENO scheme was developed for the task.

Thus, the penalty function method based on characteristics has proven its effectiveness and can be proposed for further use in numerical modeling of aerodynamic problems.

REFERENCES

- Engels T., Kolomenskiy D., Schneider K., Sesterhenn J. Numerical simulation of fluid–structure interaction with the volume penalization method. *J. Comput. Phys.*, 2015, vol. 281, pp. 96–115.
- Riahi H., Meldi M., Favier J., Serre E., Goncalves da Silva E. A pressure-corrected Immersed Boundary Method for the numerical simulation of compressible flows, 2018.

- 3 Liu Q., Vasilyev O.V. Brinkman penalization method for compressible flows in complex geometries. *J. Comput. Phys.*, 2008, vol. 227, pp. 946–966.
- 4 Fedkiw R. Coupling an Eulerian fluid calculation to a Lagrangian solid calculation with the ghost fluid method. *J. Comput. Phys.*, 2002, vol. 175, pp. 200–224.
- 5 Jost A.M.D., Glockner S. Direct forcing immersed boundary methods: Improvements to the Ghost-Cell Method, 2021.
- 6 Peskin C.S. The immersed boundary method. *Acta Numer.*, 2002, vol. 11, pp. 479–517.
- 7 Saiki E.M., Biringen S. Numerical simulation of a cylinder in uniform flow: Application of a virtual boundary method. *J. Comput. Phys.*, 1996, vol. 123 (2), pp. 450–465.
- 8 De Palma P., de Tullio M.D., Pascazio G., Napolitano M. An immersed-boundary method for compressible viscous flows. *Comput. Fluids.*, 2006, vol. 35(7), pp. 693–702.
- 9 Abalakin I.V., Zhdanova N.S., Kozubskaya T.K. Immersed boundary method as applied to the simulation of external aerodynamics problems with various boundary conditions. *Dokl. Math.*, 2015, vol. 91, pp. 178–181.
- 10 Angot P., Bruneau C.H., Fabrie P. A penalization method to take into account obstacles in viscous flows. *Numerische Mathematik*, 1999, vol. 81, pp. 497–520.
- 11 Feireisl E., Neustupa J., Stebel S. Convergence of a Brinkman-type penalization for compressible fluid flows. *Journal of Differential Equations*, 2011, vol. 250, pp. 596–606.
- 12 Wang A.-B., Trávníček Z., Chia K.-C. On the relationship of effective Reynolds number and Strouhal number for the laminar vortex shedding of a heated circular cylinder. *Physics of Fluids*, 2000, vol. 12, pp. 1401–1410.
- 13 Tritton D. Experiments on the flow past a circular cylinder at low Reynolds numbers. *J. Fluid Mech.*, 1959, vol. 6, pp. 547–567.
- 14 Williamson C.H.K. Oblique and parallel modes of vortex shedding in the wake of a circular cylinder at low Reynolds numbers. *J. Fluid Mech.*, 1989, vol. 206, pp. 579–627.
- 15 Braza M., Chassaing P., Ha Minh H. Numerical study and physical analysis of the pressure and velocity fields in the near wake of a circular cylinder. *J. Fluid Mech.*, 1986, vol. 165, pp. 79–130.
- 16 Henderson R.D. Details of the drag curve near the onset of vortex shedding. *Phys. Fluids*, 1995, vol. 7, p. 2102.
- 17 Karniadakis G.E., Triantafyllou G.S. Three-dimensional dynamics and transition to turbulence in the wake of bluff objects. *J. Fluid Mech.*, 1992, vol. 238, pp. 1–30.
- 18 Mittal R., Balachandar S. Effect of three-dimensionality on the lift and drag of nominally two-dimensional cylinders. *Phys. Fluids*, 1995, vol. 7, p. 1841.
- 19 Persillon H., Braza M. Physical analysis of the transition to turbulence in the wake of a circular cylinder by three-dimensional Navier–Stokes simulation. *J. Fluid Mech.*, 1998, vol. 365, pp. 23–88.
- 20 Abalakin I.V., Zhdanova N.S., Kozubskaya T.K. Immersed Boundary Method Implemented for the Simulation of an External Flow on Unstructured Meshes, *Mat. Model.*, 2015, vol. 10, pp. 5–20.
- 21 Edwards W.S., Tuckerman L.S., Friesner R.A., Sorensen D.C. Krylov methods for the incompressible Navier–Stokes equations. *J. Comp. Phys.*, 1994, vol. 110, pp. 82–102.
- 22 Abalakin I.V., Vasilyev O.V., Zhdanova N.S., Kozubskaya T.K. Characteristic Based Volume Penalization Method for Numerical Simulation of Compressible Flows on Unstructured Meshes. *Comput. Math. and Math. Phys.*, 2021, vol. 61(8), pp. 1315–1329.
- 23 Al-Marouf M., Samtaney R. A versatile embedded boundary adaptive mesh method for compressible flow in complex geometry. *J. Com. Phys.*, 2017, vol. 337, pp. 339–378.

^{1*}Манапова А.Қ.,

қолданбалы математика және информатика магистрі, ORCID ID: 0000-0003-1548-7061,
e-mail: manapova.a.k.math@gmail.com

²Бекетаева А.О.,

физ.-мат.ф.д., ORCID ID: 0000-0003-4360-3728,
e-mail: azimaras10@gmail.com

^{3,4}Макаров В.В.,

т.ф.к., ORCID ID: 0000-0003-4874-5418,
e-mail: makfone@mail.ru

¹Азаматтық авиация академиясы, Алматы қ., Қазақстан

²Математика және математикалық модельдеу институты, Алматы қ., Қазақстан

³РҒА Басқару мәселелері институты, Мәскеу қ., Ресей

⁴«МИФИ» Ұлттық ядролық зерттеу университеті, Мәскеу қ., Ресей

ЦИЛИНДРДІ ДЫБЫСҚА ДЕЙІНГІ СЫҒЫЛАТЫН АҒЫНМЕН АҒЫНДАУДАҒЫ АЙЫП ФУНКЦИЯЛАР ӘДІСІ

Андатпа

Қозғалатын қатты денелердің айналасындағы сығылатын ағындарды сандық модельдеу аэродинамикалық флютер, зымыран қозғалтқыштары және шассилер сияқты инженерлік қолданбаларда маңызды рөл атқарады. Айып функциялар әдісі соңғы айырмашылықтар әдісінің шеңберінде ортогональды құрылымдық торларды пайдаланған кезде тиімділігімен ерекшеленеді және ламинарлы, сондай-ақ турбулентті ағын мәселелерін шешуде кеңінен қолданылады. Бұл әдіс шекаралық шарттарды жанама түрде енгізу мүмкіндігін қамтамасыз ететін қосымша көздермен толықтырылған Навье-Стокс теңдеулерін тікелей қолдануға негізделген. Айып функциялар әдісі Дирихле шекаралық шарттарын енгізуді жеңілдетеді, бірақ Нейман шарттарын қолдануда белгілі бір қиындықтар тудыруы мүмкін. Дегенмен, әдіс шекаралық шарттардың екі түрімен де тиімді жұмыс істейді, бұл оны термиялық және сығылатын ағындар сияқты Нейман шарттары жиі қолданылатын қолданбалар үшін ыңғайлы етеді. Икемділігіне қарамастан, әдіс деректерді басқарудың жоғары деңгейін және қосымша кодтау әрекеттерін қажет етеді. Бұл мақалада сығылатын субсоникалық ағындарды сандық модельдеуде дәл нәтижелер беретін жақында әзірленген жоғары ретті әдіс қарастырылады. Әдіс Рейнольдс пен Мах сандарының кең диапазонында қозғалмайтын және қозғалатын объектілерде сыналды, бұл оның тиімділігі мен қолдану аясын көрсетеді.

Тірек сөздер: сандық модельдеу, цилиндр, дыбысқа дейінгі ағын, айып функциялар әдісі, Навье-Стокс теңдеулер жүйесі.

^{1*}Манапова А.К.,

магистр прикладной математики и информатики, ORCID ID: 0000-0003-1548-7061,
e-mail: manapova.a.k.math@gmail.com

²Бекетаева А.О.,

докт. физ.-матем. наук, ORCID ID: 0000-0003-4360-3728,
e-mail: azimaras10@gmail.com

^{3,4}Макаров В.В.

канд. техн. наук, ORCID ID: 0000-0003-4874-5418,
e-mail: makfone@mail.ru

¹Академия гражданской авиации, г. Алматы, Казахстан

²Институт математики и математического моделирования, г. Алматы, Казахстан

³Институт проблем управления РАН, г. Москва, Россия

⁴Национальный исследовательский ядерный университет «МИФИ», г. Москва, Россия

МЕТОД ШТРАФНЫХ ФУНКЦИЙ ДЛЯ МОДЕЛИРОВАНИЯ ОБТЕКАНИЯ ЦИЛИНДРА ДОЗВУКОВЫМ СЖИМАЕМЫМ ПОТОКОМ

Аннотация

Численное моделирование сжимаемых потоков вокруг движущихся твердых тел важно для таких инженерных приложений, как аэродинамический флаттер, ракетные двигатели и шасси. Метод штрафных функций особенно эффективен при использовании ортогональных структурных сеток в рамках схемы конечных разностей и широко применяется для решения задач как ламинарного, так и турбулентного течения. Метод основан на прямом применении уравнений Навье-Стокса с добавленными источниками, что позволяет задавать граничные условия косвенным образом. Этот метод облегчает наложение граничных условий Дирихле, но усложняет применение условий Неймана. Тем не менее метод хорошо работает с обоими типами граничных условий, что делает его подходящим для тепловых и сжимаемых потоков, где часто используются условия Неймана. Несмотря на свою гибкость, метод требует высокой степени управления данными и дополнительного кодирования. В данной работе представлены результаты недавно разработанного метода более высокого порядка для сжимаемых дозвуковых потоков, демонстрирующие точное моделирование движущихся объектов без численного шума. Метод был протестирован на стационарных и движущихся объектах в широком диапазоне чисел Рейнольдса и Маха.

Ключевые слова: численное моделирование, цилиндр, дозвуковое течение, метод штрафных функций, система уравнений Навье-Стокса.

Article submission date: 02.08.2024